

Supporting Information for:

Transmembrane Potential across Single Conical Nanopores and the Resulting Memristive and Memcapacitive Ion Transport

Dengchao Wang, Maksim Kvetny, Juan Liu, Warren Brown, Yan Li, and Gangli Wang*.

Department of Chemistry, Georgia State University, Atlanta, GA, 30302, glwang@gsu.edu

Experimental Details

Figure SI-1: The i - V curves and impedance spectra of the 45 nm-radius nanopore in different KCl concentrations.

Figure SI-2 : The i - V curves of a 60 nm-radius nanopore in different potential limit (> 400 mV) at scan rate of 1 V/s.

Figure SI-3: The i - V responses of a solid-state resistor-capacitor circuit at different scan rates.

Figure SI-4: Fitting model, results and illustration of the experimental data (symbols) with the fitted curves with the model.

Figure SI-5: The i - V curves of an 200 nm-radius nanopore at different scan rates in (a) 1, (b) 5, (c) 10 and (d) 50 mM KCl.

Figure SI-6: The i - V curves of an 80 nm-radius nanopore at different scan rates in (a) 1, (b) 10, (c) 50 and (d) 100 mM KCl.

Figure SI-7: The dependence of the cross-point potential on Ag/AgCl electrodes and measurement conditions.

Figure SI-8: The correlation of cross-point potential and electrolyte concentration of different sized nanopores.

Figure SI-9: Typical charging and discharging of a solid state capacitor (1 nF) in parallel with a resistor (500 M Ω).

Experiment Details:

Materials. Pt wire (25 μm diameter), silver wire (99.9985%, 0.5 mm diameter), and silver conductive paste from Alfa Aesar were used as received. CaCl_2 , H_2SO_4 , HNO_3 , H_2O_2 (30%) and acetone are from Sigma-Aldrich. Water ($\sim 18.2 \text{ M}\Omega\text{-cm}$) was purified with a Barnstead E-pure water purification system. CORNING 8161 glass capillaries (OD = 1.50 mm, ID = 1.10 mm, Warner Instruments) were used.

1. Preparation of conical nanopore membrane.

The glass nanopores are fabricated followed the reported procedures. Briefly, one end of the Pt wire is first attached to a tungsten rod for easy handling. The other end of the Pt wire (length : 2 cm, radius: 25 μm) was electrochemically etched into a sharp tip using a waveform of 300 Hz at $\sim 4 \text{ V}$ peak to peak amplitude (BK Precision 4003A function generator). After sequencing washed in piranha solution and nanopure water, the sharpened Pt tip was sealed into a glass capillary by thermo-melting. This sealing process was monitored by an optical microscope (American Scope, USA) to ensure shallow sealing depth for removal of Pt tip. The Pt tip is exposed by mechanical polishing the sealed end (Buehler Microcut paper discs 400-1200 GRIT). After the Pt tip is exposed, further electrochemical etching and subsequent mechanical pulling were performed to remove the Pt from the glass shroud. The final product is a glass membrane at the end of a glass capillary, with a conical-shaped pore replicating the geometry of the Pt tip.

2. Electrochemical Measurements

The current-voltage responses and AC impedance spectra of the prepared glass nanopore membranes were studied with the potentiostat Reference 600 from Gamry Inc. In impedance measurements, the amplitude of the AC waveform was set to 10 mV. The frequency range was in general from 500 mHz to 1 MHz.

Two Ag/AgCl wires were used as the inside and outside electrodes. The bias polarity is defined by electrode potentials outside versus inside the nanopore. The KCl solution at the same concentration was used as electrolyte both inside and outside of the glass nanopore. The orifice radius (r) of the nanopore was calculated from the conductivity equation following previously described procedure (*Anal. Chem.* **2007**, *79*, 4778 and references therein). From the almost linear i - V curve, the absolute current values at $\pm 0.050 \text{ V}$ in 1M KCl solution were used. The calculation equation is expressed as:

$$R_p = \frac{1}{\kappa r} \left(\frac{1}{\pi \tan \theta} + \frac{1}{4} \right)$$

where R_p is the resistance, κ is the conductivity of the solution, and θ is the half-cone angle.

Figure SI-1. The i - V curves and impedance spectra of the 45 nm-radius nanopore in different KCl concentrations. Panel (a), (b), and (c) present the i - V curves at different scan rates in 50, 100 and 1000 mM KCl respectively. The cross-point potential can be better seen from the enlarged insets in each panel. (d) impedance spectra taken above, below, and at the cross potential in 100 mM KCl in the form of Nyquist plot.

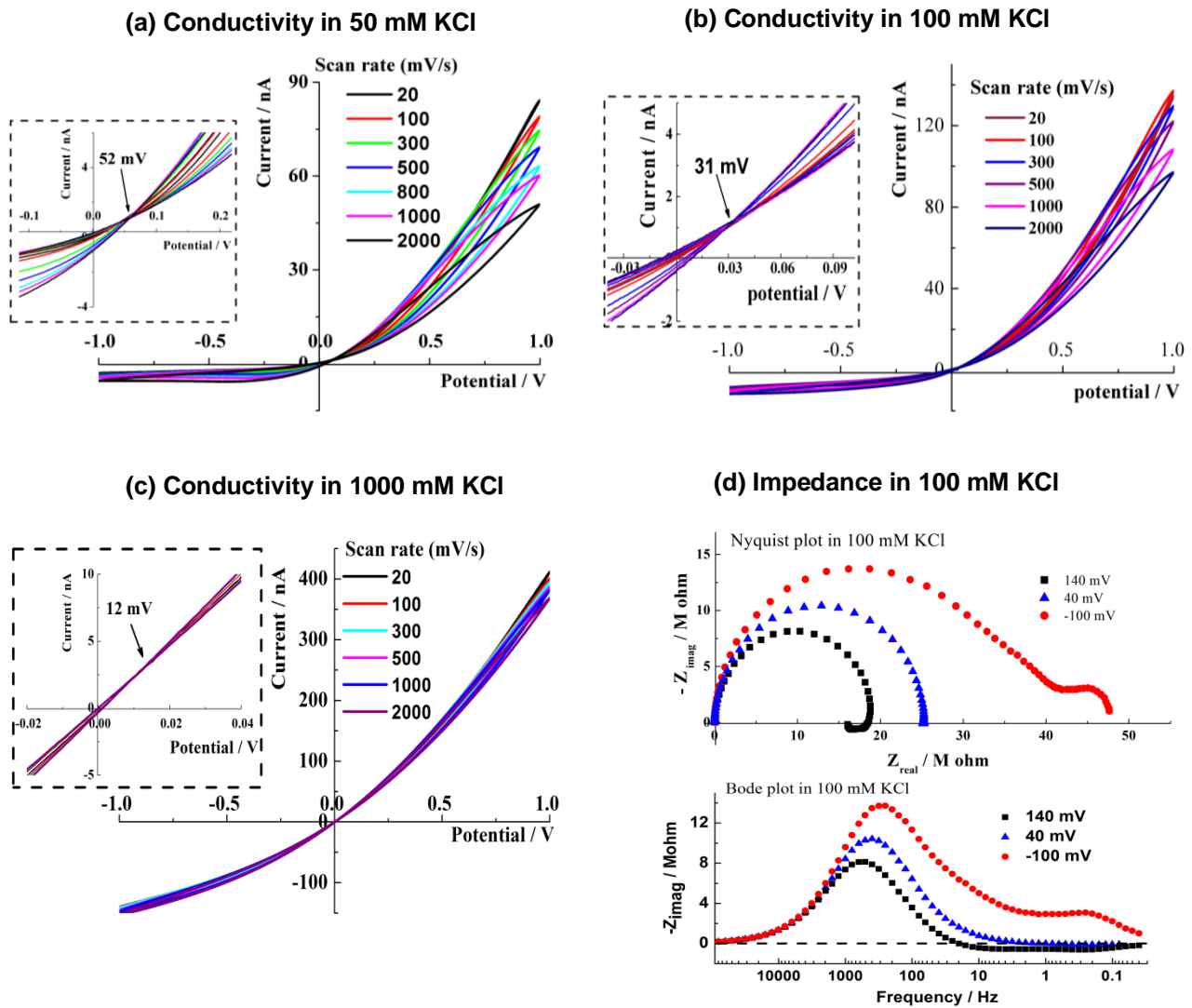


Figure SI-2: The i - V curves of a 60 nm-radius nanopore in different potential range (> 400 mV away from cross point potential) at scan rate of 1.0 V/s. The cross point potential did not change in this case. The i - V curves were shifted to demonstrate the details.

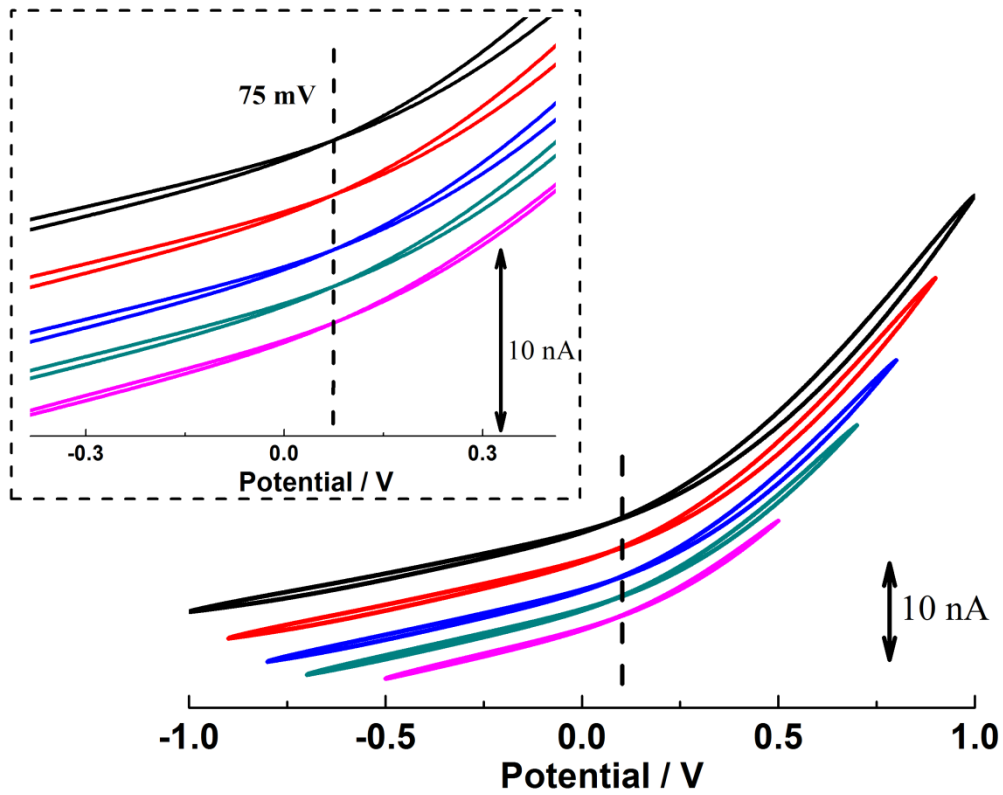


Figure SI-3. The i - V responses of a solid-state resistor-capacitor circuit at different scan rates. The arrows illustrate the direction of potential scan.

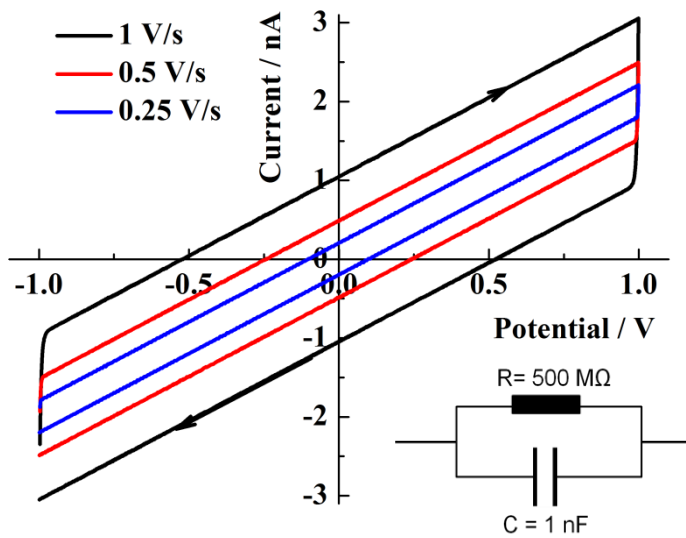
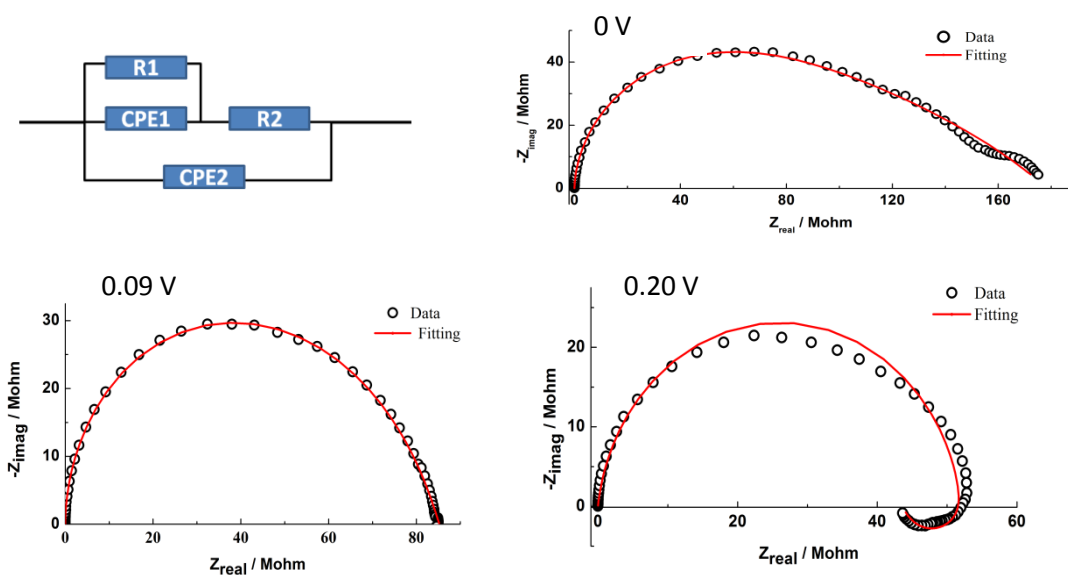


Figure SI-4: Fitting model (*Anal. Chem.* **2010**, 82, 4520) and illustration of the experimental data (symbols) with the fitted curves with the model at different bias potential. The fitting results are shown in the table below.



		CPE1	alpha		CPE2		Goodness of Fit
DC Potential / V	R1/ Ω	Y01/S*s ^a	α 1	R2/ Ω	Y02/S*s ^a	α 2	
0.20	9.37E+06	1.80E-07	-7.22E-01	4.29E+07	6.79E-12	9.70E-01	3.96E-03
0.09	4.29E+07	2.06E-10	6.73E-01	4.29E+07	5.09E-12	9.94E-01	7.74E-05
0.00	1.47E+08	6.42E-10	4.11E-01	3.11E+07	4.79E-12	9.99E-01	1.00E-04

Figure SI-5. The i - V curves of an 200 nm-radius nanopore at different scan rates in (a) 1, (b) 5, (c) 10 and (d) 50 mM KCl. The cross-point potential can be better seen from the enlarged insets in each panel.

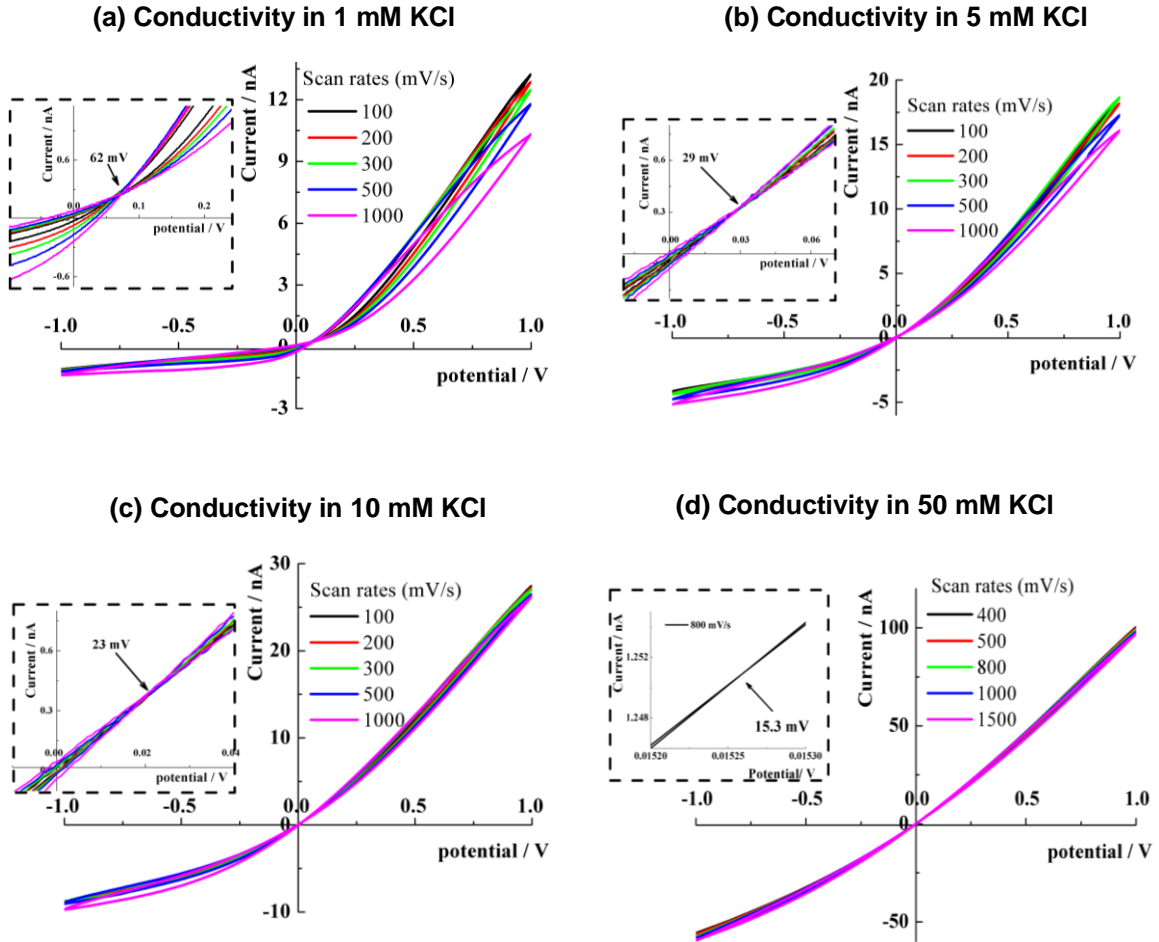


Figure SI-6. The i - V curves of an 80 nm-radius nanopore at different scan rates in (a) 1, (b) 10, (c) 50 and (d) 100 mM KCl. The cross-point potential can be better seen from the enlarged insets in each panel.

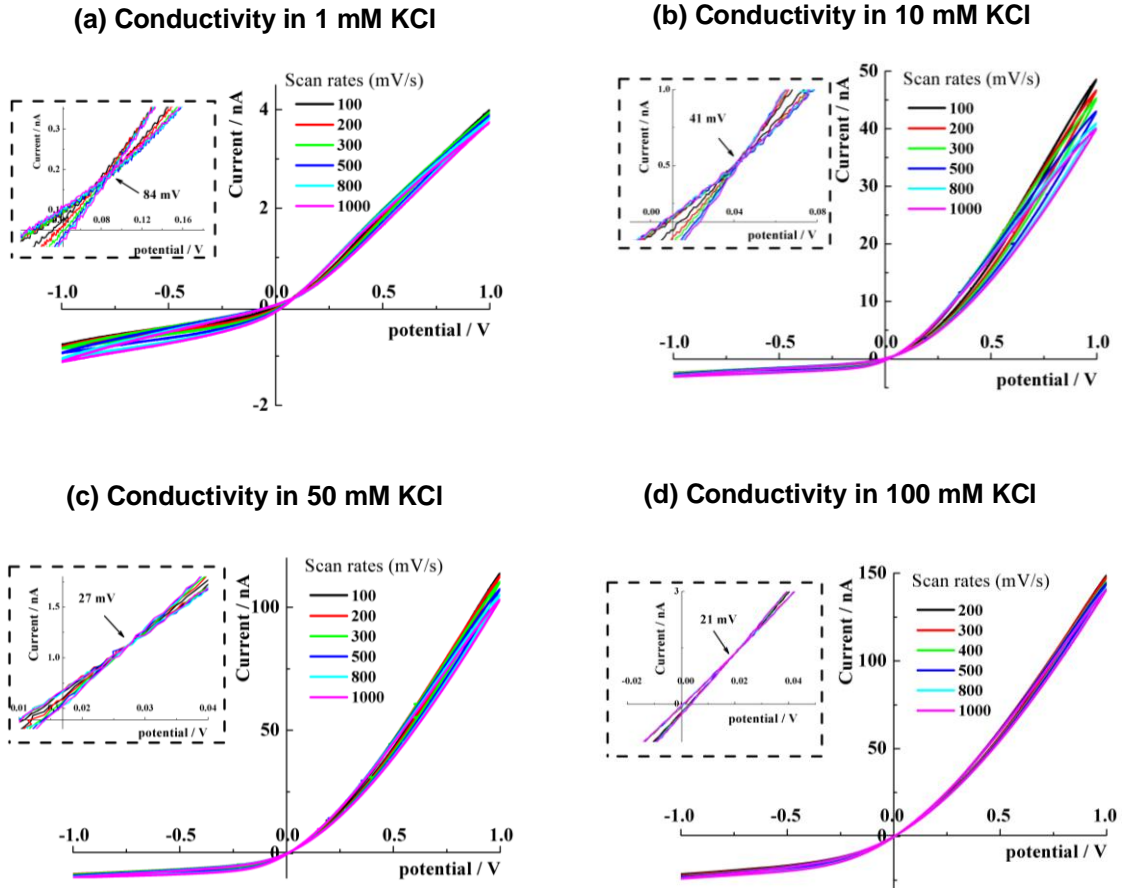


Figure SI-7. The dependence of the cross-point potential on Ag/AgCl electrodes and measurement conditions. Two i - V curves were collected before and after switching the inside and outside Ag/AgCl electrodes. A 45 nm-radius nanopore in 100 mM KCl was used. The results with 300 mV/s scan rate were presented. The inset shows zoom-in view near the crossing-point potential. The non-zero crossing behavior remains, indicating an intrinsic property of the nanopore instead of instrumental or measurement artifact. The small shift is 7 mV in these measurements. This shift is at ca. 5-10 mV in general, which is attributed to thermal fluctuation and/or the asymmetry of the two Ag/AgCl electrodes.

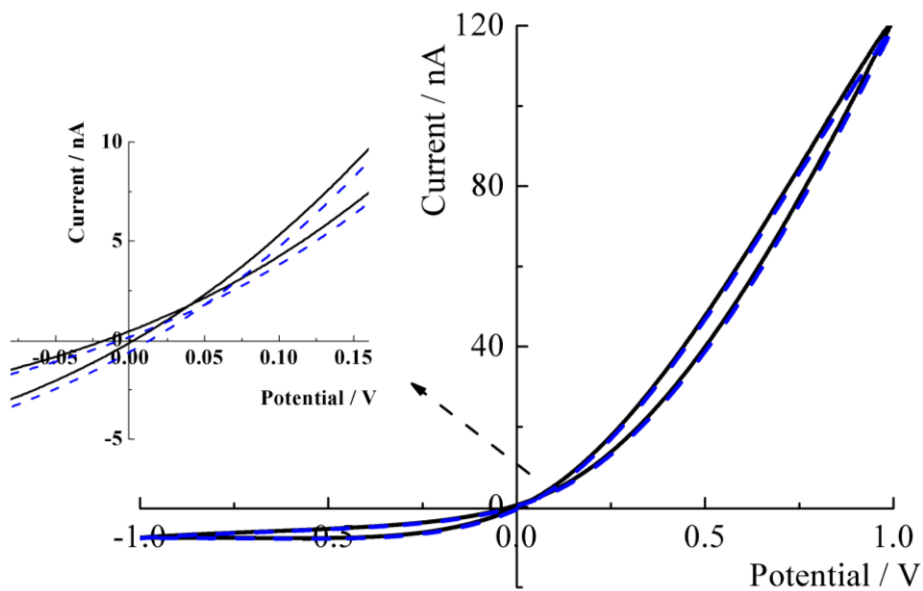
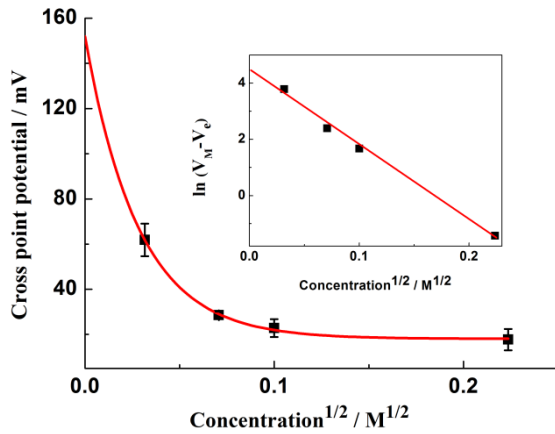


Figure SI-8. The correlation of cross-point potential and electrolyte concentration of different sized nanopores. (a) 200 nm-radius nanopore. (b) 80 nm-radius nanopore. In each concentration, the cross point potential was averaged from the i - V curves with scan rates ranging from 100 to 2000 mV/s. The nature logarithm format is plotted as inserted. The intercept V_0 is about 150 mV for the 200 nm-radius nanopore and 115 mV for the 80 nm-radius nanopore.

(a) 200 nm-radius nanopore ($V_0 = 150$ mV)



(b) 80 nm-radius nanopore ($V_0 = 115$ mV)

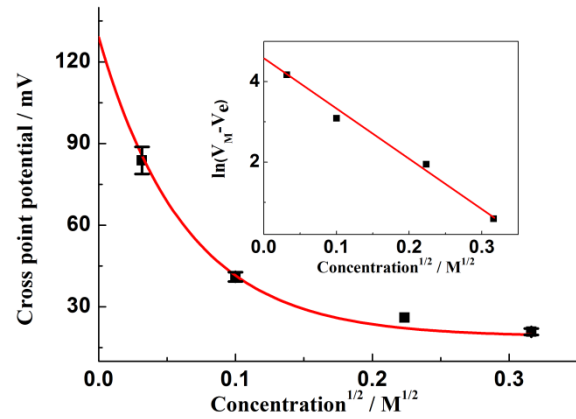


Figure SI-9. Typical charging and discharging of a solid state capacitor (1 nF) in parallel with a resistor (500 M Ω). The circuit is shown as an inset. (a) The relationship of instantaneous charges with the applied potential. The arrows indicate the direction of potential sweeping. (b) Capacitance-potential correlation. The capacitance calculated directly from $C = Q/E$ at each potential. The red line shows the zero capacitance. It is worth pointing out that the shape of the capacitance plot is symmetric and no memory effect is observed.

